Construction and Building Materials 246 (2020) 118415

Contents lists available at ScienceDirect

Construction and Building Materials

journal homepage: www.elsevier.com/locate/conbuildmat

Review

Review on geotechnical engineering properties of sands treated by microbially induced calcium carbonate precipitation (MICP) and biopolymers

Sun-Gyu Choi [a], Ilhan Chang [b], Minhyeong Lee [c], Ju-Hyung Lee [d], Jin-Tae Han [d], Tae-Hyuk Kwon [c,*]

[a] Disaster Prevention Research Division, National Disaster Management Research Institute, Ulsan, Republic of Korea
[b] School of Engineering and Information Technology, University of New South Wales (UNSW), Australia
[c] Department of Civil and Environmental Engineering, Korea Advanced Institute of Science and Technology (KAIST), Daejeon, Republic of Korea
[d] Korea Institute of Civil Engineering and Building Technology (KICT), 238 Goyangdae-ro, Ilsanseo-gu, Goyang, Republic of Korea

HIGHLIGHTS

- Biological soil improvement methods using MICP and biopolymers are reviewed.
- Engineering properties of MICP- and biopolymer-treated sands are compiled.
- Potential applications of MICP and biopolymer treatment are discussed.

ARTICLE INFO

Article history:
Received 10 January 2019
Received in revised form 9 February 2020
Accepted 12 February 2020
Available online 22 February 2020

Keywords:
Microbially induced calcite precipitation
Biopolymer treatment
Engineering properties
Calcium carbonate
Biopolymers

ABSTRACT

This study reviews the fundamental mechanisms of biological soil improvement methods—microbially induced calcium carbonate precipitation (MICP) and biopolymer treatment (BPT). Extensive experimental data on various geotechnical properties of sands treated by MICP and BPT are compiled, including the unconfined compressive strength, Mohr-Coulomb shear strength parameters, and permeability. Furthermore, the variations in these engineering parameters are correlated to calcium carbonate content for MICP and biopolymer content for BPT, which provides insights into the extent of biological modification in engineering properties of sands, potential applications, and limitations.

Contents

* Corresponding author.
E-mail address: t.kwon@kaist.ac.kr (T.-H. Kwon).

https://doi.org/10.1016/j.conbuildmat.2020.118415
0950-0618/

1. Introduction

Soil improvement is one of the most important issue in geotechnical engineering practices; cement-based materials have been widely used for various soil improvement strategies [1,2] because of their benefits such as safety, workability, and affordability. However, demand for alternative materials to cement is increasing because of its contribution to carbon dioxide (CO_2) and nitrogen oxide (NO_x) emission during production processes [3–5].

In soils, there are humongous amounts of living organisms, including bacteria, archaea, fungi, and worms. For instance, 1 kg natural soil generally contains>1 billion bacteria (>10^9 cells per kg of soil). These microorganisms in soils can generate various biochemical products such as biofilms, various gases (e.g., N_2, CO_2, NO, H_2, H_2S), biopolymers, or biominerals. Therefore, direct use of in situ microbial activities or *ex situ* microbial products has been proposed as a potential soil improvement method with low environmental impact [6,7]. Bio-mediated or bio-based soil improvement methods can be categorized based on the microbial activities or biomaterials to be exploited. These microbial activities include biomineralization, biofilm formation, biogas generation, and biopolymer/EPS accumulation; and the bio-materials exploited include food wastes such as hard shell and dairy products (e.g., casein), and biopolymers, such as gellan gum, guar gum, chitosan, glucan, and xanthan. These representative bio-mediated methods are briefly summarized as follows.

- *Microbially induced calcium carbonate (or calcite) precipitation (MICP).* This method deploys the bacterial activity that decomposes urea into carbonate and ammonium ions. The carbonate ions (CO_3^{2-}) combine with calcium ions (Ca^{2+}) to form calcium carbonate ($CaCO_3$) and the precipitated calcium carbonate can cement sand grains. The mineralogy of the precipitated calcium carbonate mostly proves to be calcite. The MICP method has been investigated for improving various soil properties, including strength and stiffness [8,9], liquefaction resistance [10,11], wind/water erosion control [12], and permeability [13,14].
- *Enzyme-induced calcium carbonate precipitation (EICP).* This method relies on the same chemical reaction involved in the MICP to form calcium carbonate. Meanwhile, the EICP method does not use bacteria; instead, it uses the enzymes extracted from bacterial solutions or plants [15,16]. The EICP method has been investigated for various purposes, including crack healing of mortars [17], protection against wind-driven erosion [18], fugitive dust control [19], and soil improvement [20,21].
- *Microbial biopolymer accumulation.* This method stimulates the microbes to produce biopolymers in soils. For instance, *Leuconostoc mesenteroides* are known to produce insoluble polysaccharide biopolymers when they are fed sucrose-rich media [22]. They decompose sucrose into fructose and glucose, and form polysaccharides linked with glucosidic bonds, referred to as dextran. This bacterial biopolymer dextran produced by *L. mesenteroides* is reported to readily reduce permeability and increase erosion resistance [23–25].
- *Biofilm formation.* Biofilms are the mixture of microbial cells and self-produced extracellular polymeric substances (EPS), and they are spontaneous and ubiquitous in natural environments. While biofilms protect microorganisms from physical, chemical, and biological external stimulations [26], biofilm formation in soils has profound effects on the formation and stability of soil bonding [27], weathering of minerals [28], degradation and sequestration of organic carbon [29], and hydraulic conductivity reduction [30–32].
- *Biogas generation.* This method exploits the microbial production of insoluble gas bubbles, including nitrogen gas and carbon dioxide gas, in water-saturated soils [33,34]. It causes partial saturation of soils, thus, it is reported to improve liquefaction resistance [33,35].
- *Biopolymer treatment* (BPT). This method refers to a technique that applies biopolymers as a chemical cementing agent to soils. The biopolymers include xanthan gum, gellan gum, beta-glucan produced by bacteria, gum from algae, guar gum from plants, chitosan from shellfish, and casein from dairy agar products [36]. For BPT, the extracted biopolymers from various sources are purified and dried, and in dry powder form, they are mixed with water and soils at a pre-determined ratio to achieve the targeted engineering performance. The BPT method can be used to increase the liquid limit and strength of soils [37,38], decrease hydraulic conductivity, improve erosion resistance, and modify water repellence [39].

Among these potential bio-based soil improvement methods, MICP and BPT have been intensively investigated to quantify the extent to which they modify various engineering properties; they are at the forefront of field-scale applications. However, adequate experimental data is yet to be compiled and compared because of varying physical characteristics of host soils and different testing conditions; this has been hampering further advancements in developing novel but practical soil improvement methods.

Therefore, this study reviews the fundamental mechanisms and potential applications of MICP and BPT for soil improvement. The experimental data on various geotechnical properties of sands treated with MICP and BPT are complied, including unconfined compressive strength (UCS), Mohr-Coulomb shear strength parameters, and hydraulic conductivity (or permeability). Furthermore, these engineering properties of MICP-treated sands and biopolymer-treated sand are correlated to the calcium carbonate content (CCC) for MICP or to biopolymer content (BPC) for BPT. The compilations and correlations presented in this study are expected to provide insights into the extent of modification in engineering properties by such methods and eventually contribute to the development of new and novel soil improvement strategies using these bio-based materials and techniques.

2. Microbially induced calcium carbonate precipitation (MICP)

2.1. Mechanism of MICP

MICP was adopted from a naturally occurring biomineralization process, where bacteria in soils induce the precipitation of calcium

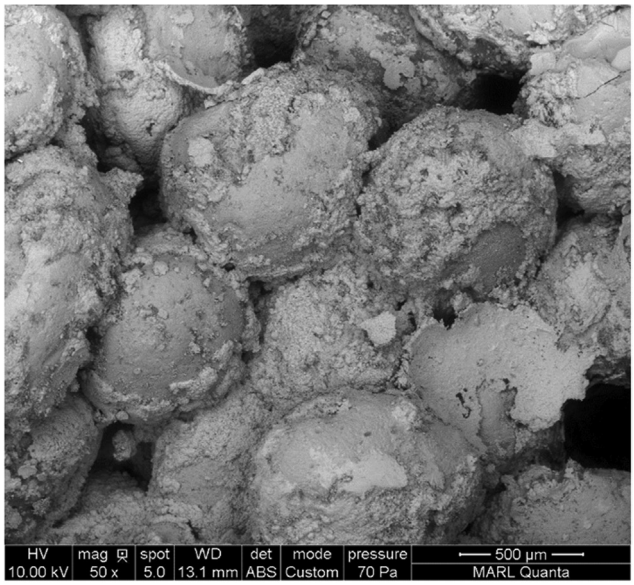

Fig. 1. SEM images of MICP-treated clean sands: (a) sand grains coated with calcite, and (b) glassbeads with precipitated calcite minerals.

Table 1
Applications of MICP methods for geotechnical engineering purposes.

Application	Microorganism	Reference
Soil stabilization/Settlement reduction	*S. pasteurii*	[8,49-53]
	Bacillus megaterium	[54]
Permeability reduction	*Bacillus* sp. *VS1*	[55]
	B. sphaericus	[56,57]
	B. megaterium	[58,59]
Erosion control	*S. pasteurii*	[61,63,64]
Liquefaction protection	*S. pasteurii*	[11,65,66]
	Soil indigenous bacteria	[67]

carbonate [40,41]. The mechanism of MICP stems from bacterial production of urease enzyme and the hydrolysis of urea [42–45]. Therefore, bacteria capable of producing urease enzyme can be used for MICP, including *Sporosarcina* strains, *Bacillus* strains, *Shewanella* strains, or Exiguobacterium strains (e.g., *Sporosarcina pasteurii*, *Bacillus subtilis*, *Bacillus sphaericus*, *Bacillus pseudofirmus*, *Shewanella alga,* or *Exiguobacterium mexicanum*). Bacteria produce urease enzyme, following which urea hydrolysis is produced by the urease enzyme, whereby urea is decomposed into ammonia (NH_3) and carbon dioxide (CO_2) (Eq. (1)). The dissolution of ammonia (NH_3) into water produces ammonium ions (NH_4^+) and hydroxide ions (OH^-), consequently increasing local pH (Eq. (2)). Meanwhile, the dissolution of carbon dioxide (CO_2) into water generates bicarbonate ions (HCO_3^-) and hydrogen ions (H^+) (Eq. (3)). In the high pH condition (or alkaline condition), this bicarbonate (HCO_3^-) reacts with the hydroxyl ions (OH^-) to form carbonate ions (CO_3^{2-}) (Eq. (4)). Hence, calcium carbonate ($CaCO_3$) is formed in the presence of calcium ions (Ca^{2+}) and soon precipitated out due to its low solubility in water (Eq. (5)).

$$CO(NH_2)_2 + H_2O \rightarrow 2NH_3 + CO_2 \quad (1)$$

$$2NH_3 + 2H_2O \rightarrow 2NH_4^+ + 2OH^- \quad (2)$$

$$CO_2 + H_2O \rightarrow HCO_3^- + H^+ \quad (3)$$

$$HCO_3^- + H^+ + 2OH^- \leftrightarrow CO_3^{2-} + 2H_2O \quad (4)$$

$$Ca^{2+} + CO_3^{2-} \rightarrow CaCO_3(s) \downarrow \quad (5)$$

As a result of urea hydrolysis, net pH increases to ~9 due to the hydroxyl ions produced during the dissolution of ammonium. Calcium carbonate minerals exist in nature as three types of anhydrous polymorphs (calcite, aragonite, vaterite); amongst the three, calcite is the most stable mineral [46]. The calcium carbonate minerals produced by MICP are mostly calcite [47]. Fig. 1 shows the SEM images of MICP-treated sands.

2.2. Potential applications of MICP

Biomineralization using the MICP method has been suggested for geotechnical engineering applications [34,48]. Thereafter, intensive and comprehensive efforts are being put into MICP. Table 1 reviews the previous studies on MICP, mainly focusing on geotechnical engineering applications [8,11,49–67].

2.3. Mechanical and hydrological properties of MICP-treated soils

The engineering properties of MICP-treated soils are affected by several environmental factors and conditions, including the injection flow rate of nutrients [68,69], chemical concentration [50,70], source of calcium ion [71,72], temperature [73,74], urease enzyme activity [73,75], pH [76], and host soil type [60,77]. Although such numerous influencing factors militate against the optimization of MICP treatments, the majority of the engineering properties of MICP-treated soils can be related to the CCC. Therefore, relationships between the CCC and various engineering properties, including the unconfined compressive strength (UCS), Mohr-Coulomb shear strength parameters (cohesion and friction angle), and permeability, are investigated based on the compiled literature data.

2.3.1. Correlation between CCC and UCS

The strength of soils treated with MICP generally increases as the amount of calcium carbonate precipitated increases; hence, the UCS has a positive relationship with the CCC [49,78–80]. Table 2 summarizes previous studies and observations on the UCS of MICP-treated soils. As mentioned earlier, while various factors

Table 2
Previous studies on UCS of MICP-treated sands.

Bacteria		Soil		Chemical concentration (Urea/Ca)	CCC (%)	UCS (kPa)	Test condition	Reference
Name	Urease activity	Type	Density (g/cm^3)					
Sporosarcina pasteurii	0.23 mS/min	Itterbeck sand	1.56	1.1/1.1	1.1 to 6.4	190 to 574	H	[83]
Sporosarcina pasteurii	1.1 mol-urea/L/h	Itterbeck sand	1.56	1.0/1.0	12.6 to 27.3	700 to 12,400	K	[84]
Sporosarcina pasteurii	0.8 to 1.2 (OD_{600})	British sand	0.2 to 1.0 (R.D)	0.1 to 1.0/0.1 to 1.0	2.6 to 9.3	37 to 2,950	A	[50]
Bacillus sphaericus	10 U/ml	Ottawa sand	1.62 to 1.63	1.0/1.0	1.14 to 13.9	180 to 2,270	I	[57]
Sporosarcina pasteurii	–	Ottawa sand	0.4 (R.D)	0.333/1.0	1.2 to 11.2	80 to 3,736	J	[85]
Bacillus sp.	10 U/ml	Silica sand (Australia)	1.60 to 1.61	1.0/1.0	1.0 to 4.0	50 to 300	G	[56]
S. pasteurii and urease	0.3 to 1.5 (OD_{600})	Ottawa sand	1.58 to 1.64	0.25 to 1.5/0.25 to 1.5	1.9 to 13.4	98 to 2,145	A, B, C, J. L	[51]
B. megaterium	$1{\cdot}10^8$ cfu/mL	Residual sand	1.52	0.25 to 1.0/0.25 to 1.0	0.7 to 2.7	67 to 140	A, B, D, F	[69]
Sporosarcina pasteurii	–	Ottawa sand	0.4 (R.D)	1.0/0.45	5.2 to 7.7	291 to 418	E	[72]
Sporosarcina pasteurii	3.7 mM/min	Ottawa sand	1.65	0.3/0.3	7.5 to 13.1	230 to 2,215	M	[52]
Bacillus sp.	10 U/ml	Silica sand (Australia)	1.63 to 1.85	1.0/1.0	1.1 to 9.4	37 to 2,112	B, C, G, J, L	[73]
Pararhodobacter sp.	–	Beachrock Sand (Japan)	–	0.1 to 0.3/0.1 to 0.3	10.7 to 28.2	495 to 9,855	A, C, D, J	[86]
Sporosarcina pasteurii	1.5 to 2.0 mL/min	Ottawa sand	1.7	0.3/0.3	6.2 to 8.9	520 to 1,709	E	[8]
Sporosarcina pastuerii		14 types	0.5 to 0.65 (R.D)	0.25 to 0.5/0.125 to 0.25	2.4 to 13.3	147 to 5,362	A, L	[87]
Pararhodobacter sp.	1 mS/ urea/min	4 types	1.49 to 1.65	0.3 to 0.7/0.3 to 0.7	10.1 to 32.0	845 to 10,000	A, C, D, J, L	[88]
S. pasteurii	0.6 to 1.2 (OD_{600})	Xiamen sand		1.0/1.0	1.4 to 9.8	48 to 1,872	B, N	[89]

Note: R.D: Relative density, OD_{600}: Optical density at 600 nm, A: Chemical Concentration, B: Urease activity, C: Temperature, D: Injection interval, E: Calcium source, F: Flow pressure, G: liquid type, H: Strength, I: Degrees of saturation, J: Treatment time, K: CCC, L: Sand, M: Fiber, N: Air.

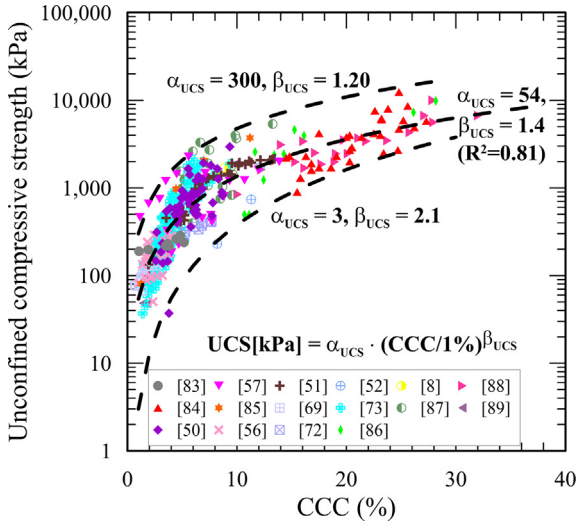

Fig. 2. Relationships between CCC and UCS.

affect the UCS of MICP-treated soils, major findings and some contradictory results can be summarized as follows:

- Lower chemical concentration induced the smaller calcite crystals, and hence, increases the UCS by a large extent [50]. However, some studies showed that 0.5 M (or 0.5 mol/L) chemical concentration (urea and calcium chloride) was the optimal concentration for the UCS [69,70].
- The effect of urease activity on the efficiency of strength improvement is still controversial. Lower urease activity was reported to be more effective in increasing the UCS due to the effective formation of cementation bridges by the slower hydrolysis of urea [73]. In contrast, it was reported that higher UCS was found with higher urease activity [51].
- Use of new calcium sources such as eggshell with vinegar [72], eggshell with hydrochloric acid (HCl) [80], and limestone with acetic acid-rich solution [8] has actively been investigated. In particular, the use of calcium acetate ($Ca(CH_3COO)_2$) as the calcium source resulted in higher strength, compared to the use of calcium chloride ($CaCl_2$), however the reason remains poorly understood [71].
- Combination of polymer fibers with MICP has also been investigated for enhancing the performance of MICP treatment by [52] and [81].
- Increases in treatment duration, repetition of treatment cycle, and chemical concentration, and a decrease in in-flow pressure are found to have positive effects on the amount degree of cementation [56,69,82].

Fig. 2 shows the compiled data on the UCS versus CCC from literatures [8,50–52,56,57,69,72,73,83–89]. It appears that the UCS ranges from 36 to 12,400 kPa, while the CCC ranges from 0.7 to 32%. A CCC of less than 1% resulted in a UCS of 36 kPa, while a CCC of 32% resulted in a UCS of 12.4 MPa, the smallest and the largest UCS values up to this point. As a positive but non-linear relation between UCS and CCC is seen, an empirical correlation between UCS and CCC can be derived as follows:

$$UCS[kPa] = \alpha_{UCS} \cdot (CCC/1\%)^{\beta_{UCS}}, \text{when } CCC < 30\%, \quad (6)$$

Table 3
Previous studies on Mohr-coulomb shear strength parameters of MICP-treated sands.

Bacteria		Soil		Properties			Test Condition	Reference
Name	Urease activity	Type	Density g/cm^3	CCC (%)	Friction angle (^{0})	Cohesion (kPa)		
Bacillus sphaericus	10 U/ml	Silica sand (Australia)	1.62–1.6339%	0.0 to 9.9	23.0 to 41.1	0.0 to 280	I, L	[57]
Sporosarcina pasteurii	0.8–1.0 OD_{600}	Ottawa sand	40%	0.0 to 5.31	33 to 43.7	–	K,	[91]
Sporosarcina pasteurii	–	Organic soil	0.6–0.69	0.0 to 16	30.0 to 38.0	8.4 to 11.0	F	[95]
Sporosarcina pasteurii	1.0 OD600	Ottawa sand	0.4, 0.75	0.0 to 4.9	33.5 to 39.5	5 to 59	K, L	[96]
Sporosarcina pasteurii	1.8 OD600	China sand		0.0 to 11.9	35.6 to 45.0	0.0 to 444.0	F, J, L	[97]

R.D: Relative density, OD_{600}: Optical density at 600 nm, A: Chemical Concentration, B: Urease activity, C: Temperature, D: Injection interval, E: Calcium source, F: Pressure, G: liquid type, H: Strength, I: Degrees of saturation, J: Treatment time, K: CCC, L: Sand, M: Fiber, N: Air.

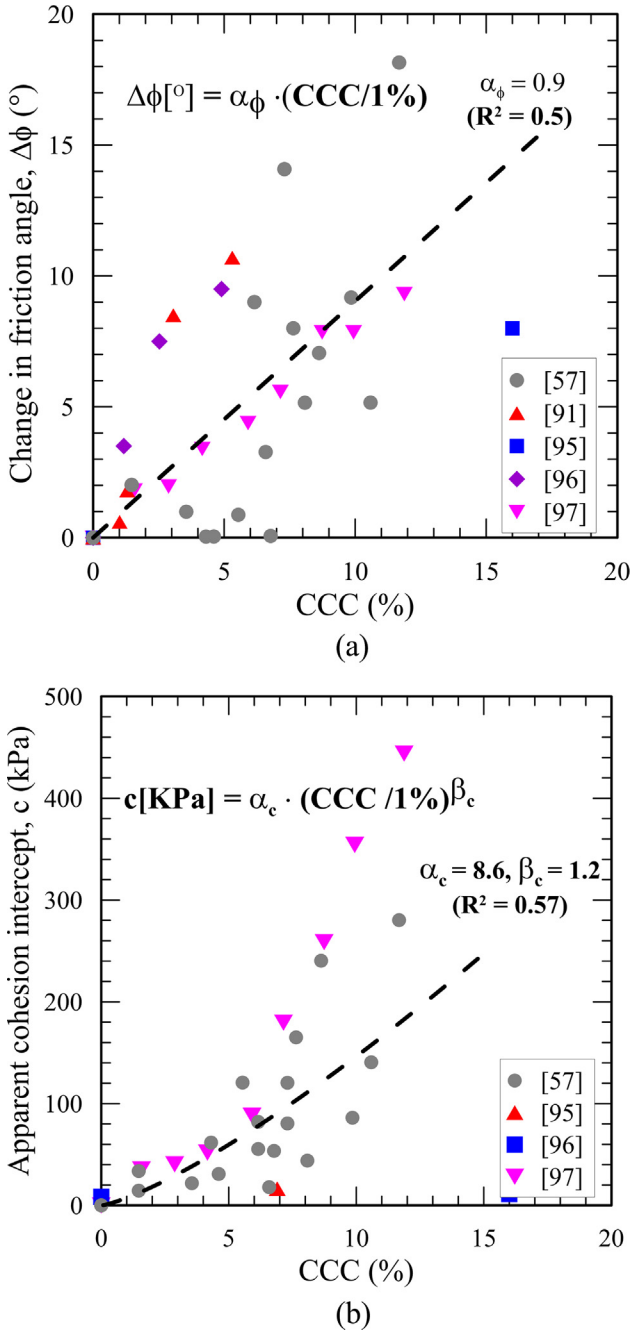

Fig. 3. Relationships: (a) CCC and change in friction angle and (b) CCC and cohesion.

where UCS is the unconfined compressive strength, CCC is the calcium carbonate content, and α_{UCS} and β_{UCS} are the empirical fitting parameters. Based on the compiled data shown in Table 2 and Fig. 2, the best-fit parameters, α_{UCS} and β_{UCS}, are determined to be 54 kPa and 1.4, respectively, using the least-square fitting method. In addition, the upper and lower bounds are drawn to include the majority of the presented data, but excluding some obvious outliers. Thereby, α_{UCS} ranges from 3 to 300 kPa, while β_{UCS} ranges from 1.2 to 2.1. Note that the empirical parameters, α_{UCS} and β_{UCS}, can differ with different MICP treatment strategies, such as microbial species, host soil type, chemical concentration, temperature, or nutrient/chemical injection method. Nevertheless, despite some scattered data, the formulation shown in Eq. (6) provides one guideline for rough estimates of the UCS for a given CCC.

2.3.2. Mohr-Coulomb shear strength parameters: Friction angle and apparent cohesion intercept

- The Mohr-Coulomb shear strength parameters—friction angle and apparent cohesion intercept—are the most widely used design parameters for describing the shear strength parameters of soils [57]. In general, the shear strength of cemented soils increases with an increase in the relative amount of the cementing agent [90], indicating the increase in the cohesion intercept and the angle of internal friction. Expectedly, the shear strength parameters were reported to increase upon the MICP treatment. In particular, the friction angles, both the peak and residual friction angles, increased with increasing CCC [91,92]. $CaCO_3$ crystals were formed at the contacts of sand grains, bonding those grains; the apparent cohesion intercept was also found to increase with the CCC [92,93]. The apparent cohesion intercept and friction angle of fine-grained swelling soils were found to increase with the cell density of bacterial solutions [94].

Table 3 shows the previous experiment data on MICP-treated sands gathered for this study [57,81,91,95–97]. The friction angles were measured to vary from 21.0 to 45.0° for a CCC varying from 0 to 16%. As the baseline friction angle prior to the MICP varies with grain size, soil type, or relative density, the change in friction angle (ϕ - ϕ_o) is plotted against the CCC, as shown in Fig. 3a, and the relationship between (ϕ - ϕ_o) and the CCC is expressed as a linear relationship, as follows:

$$\Delta\phi[^\circ] = \phi - \phi_o = \alpha_\phi(CCC/1\%), \text{when } CCC < 15\%, \quad (7)$$

where ϕ is the friction angle of the MICP-treated soil, ϕ_o is the friction angle of untreated soil, and α_ϕ is the empirical fitting parameter. The best-fit parameter, α_ϕ, is computed to be 0.90°.

Meanwhile, as shown in Fig. 3b, the apparent cohesion intercept ranges from 0 to 443.9 kPa when the CCC varies from 0 to 11.9%. Similar to what is observed with the UCS, the apparent cohesion intercept increases exponentially with increasing CCC [100]. Therefore, the cohesion-CCC relationship can be captured in a power function, as follows:

Table 4
Previous studies on permeability of MICP-treated sands.

Bacteria		Soil		Properties		Test Condition	Reference
Name	Urease activity	Type	Density g/cm^3	CCC (%)	Permeability (K, m/s)		
Sporosarcina pasteurii	0.8 to 1.2 (OD_{600})	British sand	0.2 to 1.0 (R.D)	0.0	1.98×10^{-4}	A	[50]
				8.9	1.18×10^{-6}		
Bacillus sp.	10 U/ml	Silica sand (Australia)	1.60 to 1.61	0.0*	1.30×10^{-4}	G	[56]
				4.0	4.22×10^{-5}		
Sporosarcina pasteurii	–	Ottawa sand	0.4 (R.D)	0.0*	1.0×10^{-4}	E	[72]
				7.7	1.06×10^{-6}		
Sporosarcina pasteurii	3.7 mM/min	Ottawa sand	1.65	0.0*	1.50×10^{-4}	M	[52]
				13.1	1.16×10^{-5}		
Sporosarcina pasteurii	1.5 to 2.0 mL/min	Ottawa sand	1.7	0.0*	3.00×10^{-5}	E	[8]
				8.2	1.52×10^{-6}		
Sporosarcina pasteurii	0.8 to 1.2 (OD_{600})	Sand	–	0	5.04×10^{-5}	J, M	[77]
				3.8	2.45×10^{-6}		

R.D: Relative density, OD600: Optical density at 600 nm, A: Chemical Concentration, B: Urease activity, C: Temperature, D: Injection interval, E: Calcium source, F: Pressure, G: liquid type, H: Strength, I: Degrees of saturation, J: Treatment time, K: CCC, L: Sand, M: Fiber, N: Air.
*Estimated value based on the power trend.

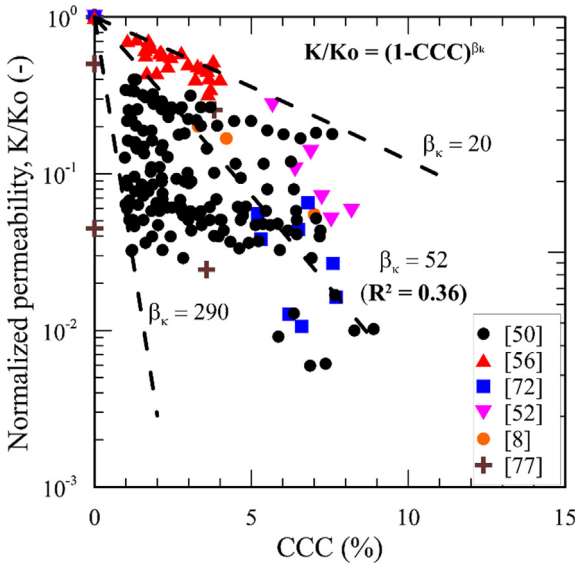

Fig. 4. Relationships of CCC and normalized permeability.

$$c[kPa] = \alpha_c \cdot (CCC/1\%)^{\beta_c}, \text{when } CCC < 15\%, \quad (8)$$

where c is the apparent cohesion intercept, and α_c and β_c are the empirical fitting parameters. Because of no or minimal cohesion of coarse-grained soils or sands, the apparent cohesion intercept prior to the MICP is determined to be zero. The best-fit parameters, α_c and β_c, are 8.6 kPa and 1.2, respectively.

2.3.3. Permeability

The produced $CaCO_3$ crystals precipitated in soils reduce the void ratio (or porosity) of the soils, causing an increase in the flow resistance and leading to the development of new preferential liquid flow paths [98]. As a result, the permeability of the soils is reduced as the carbonate crystals precipitated. The reduction in the permeability of the MICP-treated samples was mainly controlled by the amount of $CaCO_3$ precipitation, whereas, the level of the urease activity used in treatment has a minor impact [73]. For instance, significant reductions in permeability by ~50–99% were observed in various studies [58,99–101]. Particularly, it is worth noting that a fairly large amount of calcium carbonate, e.g., ~10% CCC, was required to reduce the permeability by two orders of magnitudes [102,103]. Interestingly, a remarkably slow reduction trend can be seen, compared to other cementing agents or inclusions, such as biopolymers or Portland cements. This is possibly attributable to the locations of carbonate mineral precipitated in the pores.

To examine the relationship between CCC and permeability, some experimental data were compiled from literature, as listed in Table 4 [8,50,52,56,72,77]. The permeability normalized by its baseline value prior to the MICP treatment (i.e., K/K_o) is plotted against the CCC, as shown in Fig. 4. The normalized permeability (K/K_o) can be related to the CCC, using a power function, as follows:

$$K/K_o = (1 - CCC)^{\beta_k}, \text{when } CCC < 10\%, \quad (9)$$

Table 5
Characteristics of biopolymers considered for soil improvement.

Biopolymer	Chemical composition	Main characteristics	Reference
Cellulose	*β-(1 → 4)-D-glucose* linkages	-Mostly hydrophilic -Properties depend on the chain length	[112]
Starch	*D-glucose* linked by *α-(1, 4) glucosidic bonds*	-Solubility in water depending on temperature -Used as viscosity thickeners and stabilizers	[113]
Chitosan	*P-(1,4)-2-amino-2-deoxy-D-glucose*	-Solubility increases with a decrease in pH -Cationic nature mainly binds with negatively charged surfaces	[114]
Xanthan gum	$C_{35}H_{49}O_{29}$	-Highly viscous and pseudoplastic rheology -Commonly used in drilling muds and soil treatment	[115]
Gellan gum	$C_{24}H_{37}O_{20}$	-Temperature-dependent viscosity variation (thermogelation) -Irreversible gel formation once cooled below 40 °C	[116]
Agar gum	$C_{14}H_{24}O_9$	-Reversible gelation with heating and cooling -Most common gelling agent in food	[117]
Curdlan	$(C_6H_{10}O_5)_n$	-Gel formation via heating in aqueous solutions -Applied to prevent material separation in concrete mixtures	[118]
Beta-glucan	D-glucose monomers linked by *β*-glycosidic bonds	-Capable of immune activation in humans and cholesterol absorption capabilities -Promotes vegetation growth in soils	[119,120]

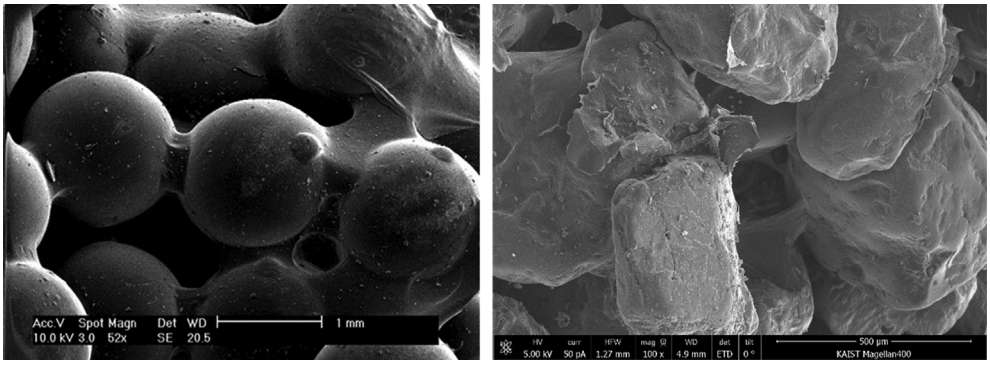

Fig. 5. SEM images of biopolymer-treated coarse particles. (a) Beta-glucan-treated silica beads [122]. (b) Gellan gum-treated silica sand [123,149].

where β_k is the empirical fitting parameter. The best-fit parameter, β_k, is calculated as 52, using the least-square fitting method. When the upper and lower bounds are drawn to include the majority of the presented data, but excluding some obvious outliers, β_k is found to range from 20 to 290 as the upper and lower bounds, as shown in Fig. 4.

The considerable scatters in those geotechnical property data plotted against CCC directly indicate that there are many other parameters affecting the geotechnical properties, such as soil particle size, shape, calcium carbonate mineralogy, fine contents and clay mineralogy if there is any, bacterial strains, temperature, curing, and aging effect (or diagenetic process). Therefore, beyond the simple formulations proposed in this study, further research is warranted to develop more generic formulations that convolute such other affecting factors.

3. Biopolymer-treated soils (BPTS)

3.1. Mechanism of BPTS

Biopolymers are organic polymers produced by biological organisms which are categorized into three major classes: polynucleotides, polypeptides, and polysaccharides [104]. Of the three, polysaccharides are the most common biopolymer type used in various industry fields, including civil and construction engineering practices [105]. Generally, polysaccharide-type biopolymers are hydrophilic due to the abundant surface hydroxyl groups (OH^-), which mainly form viscous hydrogels in the presence of water [106,107]. The viscosity (or shear modulus) of biopolymer hydrogels varies based on the biopolymer-to-water content [108,109] and presence of counter-ions (alkali- or alkali earth-metal ions) [110,111], where the increase of both variables result in higher viscosity values of biopolymer hydrogels. Table 5 lists the typical characteristics of biopolymers considered for soil improvement [112–120].

The strengthening mechanism of BPTS is governed by the rheology of biopolymer hydrogels and the chemical (ionic-, hydrogen-) bonding between biopolymers and soil particles [105], where soil type becomes an important parameter [121]. Fig. 5 shows the scanning electron microscopy (SEM) images of dried biopolymer-treated coarse soils, where mainly dehydrated biopolymer hydrogels form coats around electrically neutral silica-based particle surfaces [122,123]. For saturated conditions, biopolymer hydrogels in pore spaces are reported to increase the apparent cohesion intercept with increasing biopolymer-to-water content, while the friction angle remains constant, regardless of biopolymer content [121]. Thus, it seems that the biopolymer-to-water content and accompanying hydrogel viscosity become the main strengthening factors for coarse soils.

Table 6
Applications of BPTS methods for geotechnical engineering applications.

Application	Biopolymer	Reference
Soil strengthening	Agar gum, Starch	[38]
	Gellan gum, Agar gum	[124]
	Starch	[125]
	Casein	[126]
	Casein	[131]
	Xanthan gum	[127]
	Beta-glucan	[122]
	Xanthan gum, Guar gum	[129]
	Chitosan	[130]
Soil consistency control	Xanthan gum	[132]
	Xanthan gum, Guar gum	[133]
	Beta-glucan	[134]
	Xanthan gum	[135]
Erosion control and Surface stabilization	Xanthan gum, Chitosan	[136]
	Xanthan gum, Chitosan, Starch	[137]
	Rhizobium tropici exopolysaccharide	[138]
	Beta-glucan, Xanthan gum	[139]
	Xanthan gum	[140]
	Starch	[142]
Soil hydraulic conductivity control	Gellan gum	[123]
	Guar gum, Xanthan gum, Agar gum	[143]
	Guar gum, Xanthan gum, Chitosan	[144]
	Humic acid	[145]
Seismic resistance improvement	Xanthan gum, Gellan gum	[146]
	Agar gum	[147]

3.2. Potential applications of BPTS

In civil and construction engineering practices, biopolymers have been applied as plasticizers or viscosifiers for construction materials such as concrete mixtures, drilling fluids, and cementitious grouts. In geotechnical engineering applications, recent attempts have been made to use biopolymers as new materials for soil treatment and ground improvement.

In particular, BPTS technology shows promising functions for soil strengthening [38,122,124–131], soil consistency control via liquid limit increase [132–135], soil erosion control/reduction [136–139], ground surface stabilization [140–142], soil hydraulic conductivity control [123,143–145], and seismic resistance improvement [146,147]. Table 6 provides more details of BPTS in geotechnical engineering practices.

3.3. Mechanical and hydrological properties of BPTS

3.3.1. UCS of BPTS

Biopolymer treatment is used for various soil types; however, major emphasis is placed on clean sands, in comparison with MICP. Table 7 shows the experimental data on the UCS of BPTS and Fig. 6

Table 7
Previous studies on UCS of BPTS.

Biopolymer type	Soil type	USCS	BPC (%)	UCS (kPa)	Reference
Xanthan gum	Crushed limestone sand	SP	0.0 to 5.0	460 to 1,020	[148]
Xanthan gum	Jumunjin sand (Korea)	SP	0.5 to 1.0	370 to 880	[149]
Gellan gum	Jumunjin sand (Korea)	SP	0.5 to 1.5	13 to 435	[123]
Xanthan gum	Mine tailing (USA)	SM	0.0 to 0.5	241 to 514	[150]
Xanthan gum	SandAl-Sharqia desert sand (Oman)	SP	0.0 to 5.0	15 to 1,700	[151]
Xanthan gum	Narli sand	SP	0.5 to 1.5	1,132 to 2,109	[152]
Xanthan gum	Warsaw sand (Poland)	SP	0.5 to 1.5	1,132 to 2,109	[153]
Polyurethane resin	Nanjing sand (China)	SP	0.0 to 5.0	62 to 356	[154]
Casein, Sodium caseinate	Dune sand (Kerman, Iran)	SP	0.0 to 5	21 to 1,709	[126]

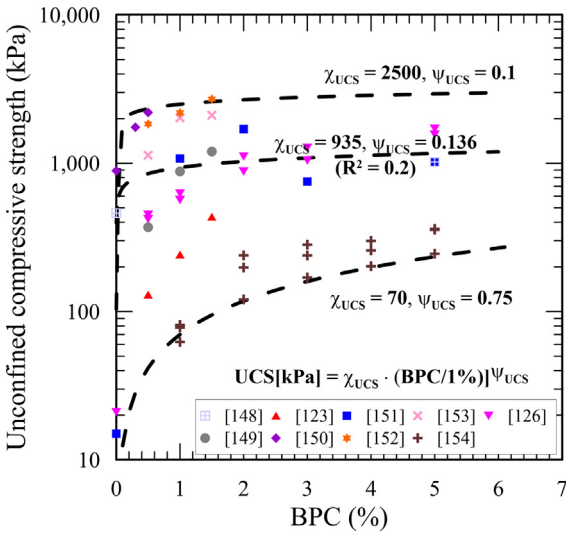

Fig. 6. Relationship between BPC and UCS.

shows the compiled data on the UCS versus BPC from literatures [123,126,148–154]. In the same manner with MICP-treated sands, a relationship between UCS and BPC is derived as follows:

$$UCS[kPa] = \chi_{UCS} \cdot (BPC/1\%)^{\psi_{UCS}}, \text{when } BPC < 5\%, \quad (10)$$

where BPC is the biopolymer content (%), defined as the mass of biopolymer divided by the dry sand mass, and χ_{UCS} and ψ_{UCS} are the empirical fitting parameters for BPTS in Fig. 6. The best-fit parameters, χ_{UCS} and ψ_{UCS}, are determined to be 935 kPa and 0.136, respectively by using the least-square fitting method. Additionally, the upper and lower bounds are drawn to include the majority of the presented data; and χ_{UCS} and ψ_{UCS} range from 70 to 2500 kPa, and 0.1–0.75, respectively. This large scatter is thought to be due to the variations in biopolymer type. It is clearly observed that UCS increases with the BPC because of inter-particle bondings induced by biopolymer hydrogels. However, it is reported that a BPC of 5% appears to be the upper most allowable BPC because a BPC greater than 5% restricts uniform biopolymer-soil mixing due to the high viscosity of biopolymer hydrogels. Meanwhile, it is worth noting that the UCS appears to approach an asymptotic value with increasing BPC, as the BPC exceeds ~3–4%. This contrasts with the MICP results, where the UCS increased exponentially with increasing BPC. For instance, the power exponent, β_{UCS}, in Eq. (6) for MICP ranges from 1.2 to 2.1, which is>1. Whereas, the power exponent, ψ_{UCS}, is less than 1, indicating the decrease in the UCS increment rate with a BPC increment.

3.3.2. Mohr-Coulomb shear strength parameters – friction angle and apparent cohesion intercept – Of BPTS

As shear strength becomes a governing design parameter for geotechnical engineering structures, various studies have been conducted on the application of biopolymers toward improving the shear strength (Friction angle and cohesion) properties of sand [126,147,150,155], as listed in Table 8. Fig. 7 shows the selected data from Table 8. The application of BPTS clearly increased the friction angle of sands, though its extent varied according to biopolymer type. As the baseline friction angle prior to biopolymer treatment varies with grain size, soil type, or relative density, the change in friction angle (ϕ - ϕ_o) is plotted against the BPC, and in the same manner with MICP, the relationship between (ϕ - ϕ_o) and BPC is expressed as a linear relationship with an empirical fitting parameter χ_ϕ, as follows:

$$\Delta\phi[^\circ] = \phi - \phi_o = \chi_\phi \cdot (BPC/1\%), \text{when } BPC < 3\% \quad (11)$$

The best-fit parameter, χ_ϕ, is determined to be 4.2°, which is much greater than the fitting parameter for MICP (i.e., α_ϕ = 0.9°). This indicates that for the same mass fraction of inclusion, whether it is calcium carbonate or biopolymer, the increment in friction angle is much greater in BPTS than in MICP-treated sands.

Table 8 also shows the experimental data on the apparent cohesion intercept of BPTS [126,147,155]. The apparent cohesion intercept was found to significantly increase by approximately 86–200 kPa for a BPC of 1–3%, and these data are plotted in Fig. 7b. Likewise, it appears that the apparent cohesion intercept exponentially increases with increasing BPC, which is the similar trend observed with the UCS. Therefore, the cohesion-BPC relationship can be captured in a power function as follows:

$$c[kPa] = \chi_c \cdot (BPC/1\%)^{\psi_c}, \text{when } BPC < 3\%, \quad (12)$$

where c is the apparent cohesion intercept, and χ_c and ψ_c are the empirical fitting parameters. Owing to no or minimal cohesion of coarse-grained soils or sands, the apparent cohesion intercept prior to biopolymer treatment is determined to be zero. The best-fit parameters χ_c and ψ_c are 90 kPa and 0.724, respectively. This

Table 8
Precious studies on Mohr-coulomb shear strength parameters of BPTS.

Biopolymer type	Soil type	USCS	BPC (%)	Friction angle (kPa)	Cohesion (kPa)	Reference
Xanthan gum	Mine tailing (USA)	SM	0.0 to 0.5	32.3 to 41.4	–	[150]
Agar gum	Sabarmati sand (India)	SM-SP	0.0 to 3.0	23.4 to 34.3	0.0 to 86.0	[147]
Xanthan gum	Jumunjin sand (Korea)	SP	0.0 to 2.0	17.5 to 38.4	13 to 218	[155]
Casein, Sodium caseinate	Dune sand (Kerman, Iran)	SP	0.0 to 1.0	36.7 to 46.0	0.17 to 145.9	[126]

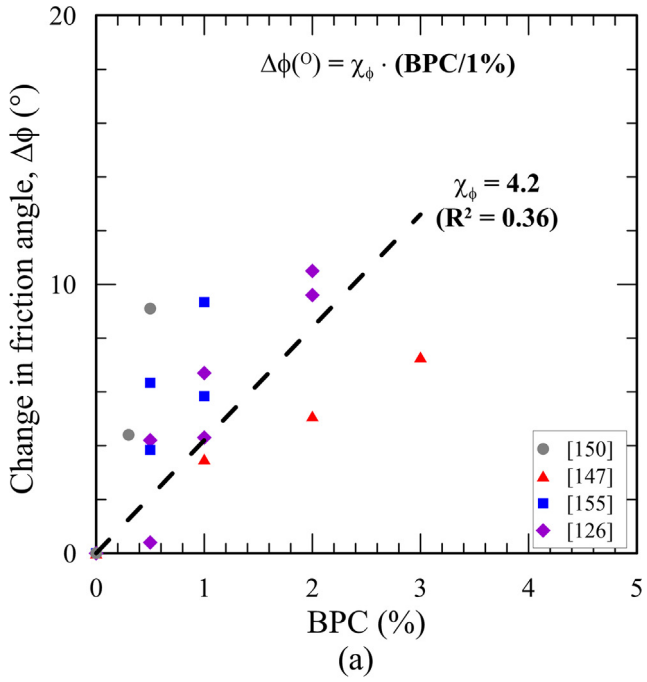

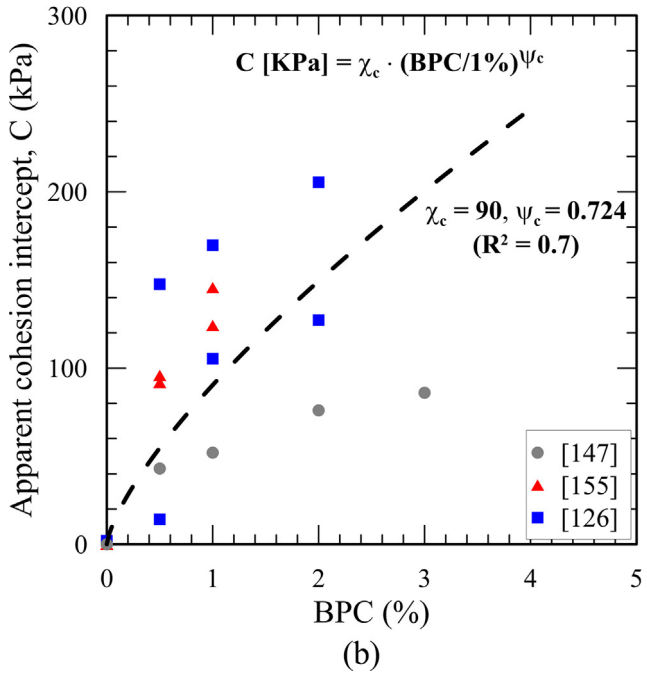

Fig. 7. Relationships: (a) BPC and change in friction angle and (b) BPC and cohesion.

demonstrates that the inter-particle cohesion increment is induced by biopolymer treatment.

A drying process involving hydrogel dehydration provides significant increase in cohesion due to the hydrogel condensation and accompanying biopolymer-induced bio-cementation [121,135]. Dried biopolymer hydrogels are transformed to thick film-like filaments, forming a continuous biopolymer matrix through inter-granular pore spaces [122,149]. These filaments with high tensile strength enhance inter-particle bonding and cohesion [123].

3.3.3. Permeability

Table 9 shows the hydraulic conductivity (or permeability) of BPTS [123,156,157]. It appears that application of biopolymer treatment readily reduced the permeability by more than 3 orders of magnitudes with less than 8% BPC. This remarkable reduction is mainly due to the pore-clogging effect induced by biopolymer hydrogels. Fig. 8 plots the permeability normalized by its baseline value prior to BPT (i.e., K/K_o) with BPC. Accordingly, the normalized permeability (K/K_o) can be related to BPC using a power function, as follows:

$$K/K_o = (1 - BPC)^{\psi_k}, \text{when } BPC < 8\%, \quad (13)$$

where ψ_k is the empirical fitting parameter. The best-fit parameter ψ_k is determined to be 314 by using the least-square fitting method, and the upper and lower bounds are 55 and 1500, respectively when drawn to include the majority of the presented data. Compared to the power exponent value for MICP (i.e., β_k = 20–290), such high ψ_k value supports the effectiveness of permeability reduction by biopolymers.

The vast scatters in the geotechnical properties against BPC are presumably attributable to the many other factors and parameters, such as soil particle size, shape, fine contents and clay mineralogy if there is any, temperature, humidity, curing condition, and aging effect. Again, development of more generic formulations is warranted beyond the simple formulations proposed in this study.

4. Comparisons of engineering properties for MICP and BPTS

In this section, the engineering properties and their correlation with the CCC/BPC of MICP-treated sands and BPTS gathered are

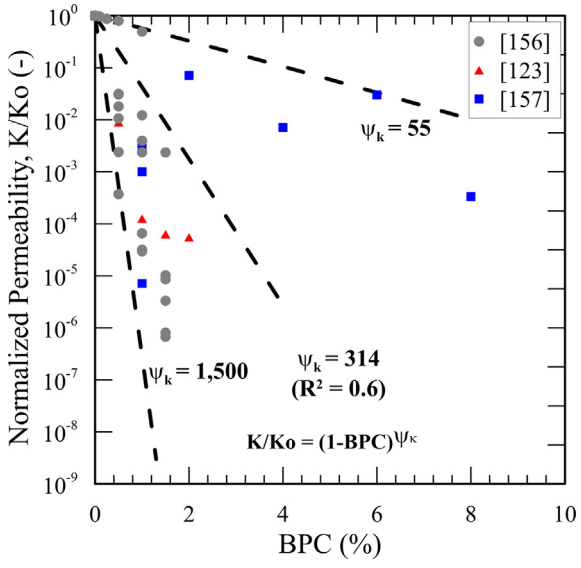

Fig. 8. Relationship between BPC and normalized permeability.

Table 9
Previous studies on permeability of BPTS.

Biopolymer type	Soil type	USCS	BPC (%)	Permeability (m/s)	K/Ko @ max BPC	Reference
Xanthan gum	Narli sand (Turkey)	SP	0.0 to 1.5	7.16×10^{-3} to 5.69×10^{-11}	~8×10^{-9}	[156]
Gellan gum	Jumunjin sand (Korea)	SP	0.0 to 2.0	2.11×10^{-6} to 2.11×10^{-10}	~10^{-4}	[123]
Guar gum	Thar desert sand (India)	SP	0.0 to 8.0	7.00×10^{-6} to 5.00×10^{-11}	~7×10^{-6}	[157]

compared. Table 10 summarizes the results of the empirical fitting parameters determined in this study.

Fig. 9a shows all the collected data for the UCS versus the CCC and BPC. It indicates that the UCS of MICP-treated sands increases continuously with the CCC. Note that the maximum CCC that has been experimentally achieved is reported to be 33%, and the pore spaces are expected to be completely filled by carbonate minerals. The maximum UCS, that is considered the upper limit, is also reported to be ~12 MPa with ~33% CCC. Whereas, the UCS of BPTS exhibits a considerable increase in UCS with the BPC lower than 1%, thereafter, the increment in UCS gradually diminishes as the BPC exceeds ~1%. The maximum UCS experimentally achieved is reported to be ~2 MPa. This is also consistent with the fitting parameter values, where the power exponents, β_{ucs} and $\psi_{ucs,}$ range from 1.2 to 2.1 and 0.1–0.75, respectively, and the parameter α_{ucs} and χ_{ucs} range from 3 to 300 kPa and 70 to 2500 kPa, respectively (Table 10).

Table 10
Empirical fitting parameters and formulations for MICP and BPTS.

Property	Type	α or χ	β or ψ	Formulation
UCS	MICP	54 kPa	1.4	$UCS[kPa] = \alpha_{UCS} \cdot (CCC/1\%)^{\beta_{UCS}}$
	BPTS	935 kPa	0.136	$UCS[kPa] = \chi_{UCS} \cdot (CCC/1\%)^{\psi_{UCS}}$
△ϕ	MICP	0.9°	–	$\Delta\phi[^\circ] = \phi - \phi_o = \alpha_\phi \cdot (CCC/1\%)$
	BPTS	4.2°	–	$\Delta\phi[^\circ] = \phi - \phi_o = \chi_\phi \cdot (BPC/1\%)$
c	MICP	8.6 kPa	1.2	$c[kPa] = \alpha_c \cdot (CCC/1\%)^{\beta_c}$
	BPTS	90 kPa	0.724	$c[kPa] = \chi_c \cdot (BPC/1\%)^{\psi_c}$
K/Ko	MICP	–	52	$K/K_o = (1 - CCC)^{\beta_k}$
	BPTS	–	314	$K/K_o = (1 - BPC)^{\psi_k}$

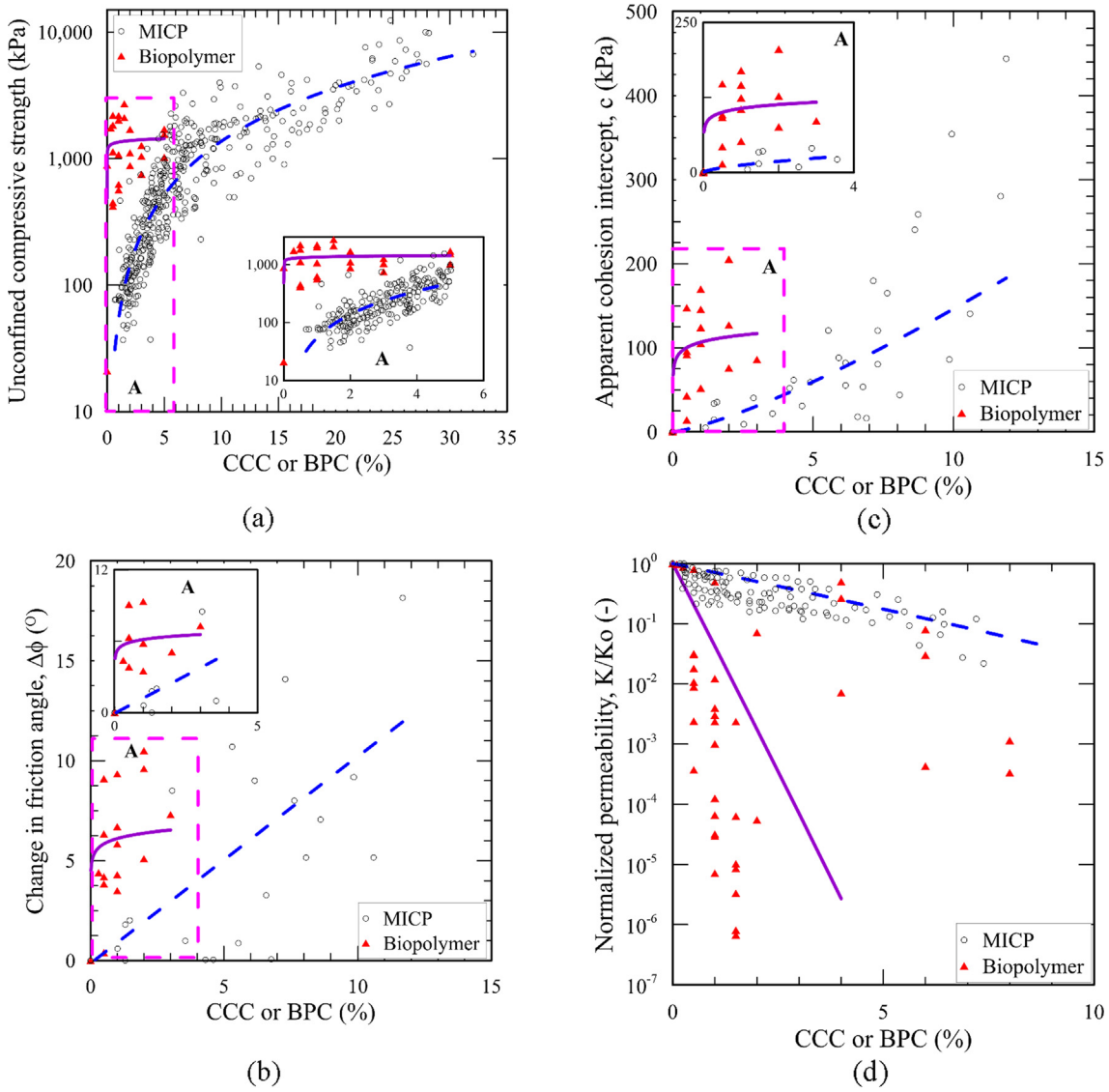

Fig. 9. Comparisons between MICP- and biopolymer-treated sands for (a) UCS, (b) change in friction angle, (c) cohesion, and (d) normalized permeability.

Fig. 9b shows all the collected data for the change in friction angle (Δ_ϕ) versus the CCC and BPC. For a given CCC or BPC, i.e., the same mass fraction of inclusion, whether it is calcium carbonate or biopolymer, the increase in the friction angle of BPTS is greater by approximately five times that of MICP-treated sands. In addition, this is consistent with the fitting parameters α_ϕ and χ_ϕ values, 0.9° and 4.2°, respectively. Fig. 9c shows all the collected data for the apparent cohesion intercept (c) versus the CCC and BPC. Similar to the UCS, the cohesion intercept of MICP-treated sands increases continuously with the CCC, with the power exponent, β_c, of 1.2 (see Fig. 9c and Table 10). Whereas, the cohesion intercept of BPTS exhibits a rapid increase at a low BPC regime thereafter, its increment gradually diminishes. This led to the power exponent, ψ_c, of 0.724. The maximum cohesion values of MICP-treated sands and BPTS are reported to be ~440 kPa and ~200 kPa, respectively.

Fig. 9d shows all the experimental results of the normalized permeability (K/K_o) versus the CCC and BPC. The power exponents, β_k for MICP and ψ_k for BPTS, are determined to range from 20 to 290 and 55 to 1500, respectively. This is one of the important and distinctive differences between MICP and BPTS. This clearly shows the effectiveness of biopolymer treatment in permeability reduction over MICP. This is attributed to the combination of the precipitation and cementing effects of calcium carbonate on sand pores and the swelling of biopolymer-hydrogels in saturated conditions. During permeability measurement, note that the specimens were water-saturated, and thus, viscous hydrogel decreases the mobility or conductance of water through the specimen. Meanwhile, carbonate minerals, mostly calcite, are precipitated on the sand grain surfaces, and thus, it appears that the precipitated calcite hardly occludes the pore throats [102,103].

5. Concluding remarks – implications and potential applications

In this study, the fundamental mechanisms of microbially induced calcium carbonate precipitation (MICP) and biopolymer treatment (BPT) and their engineering properties are reviewed by compiling and comparing extensive experimental results. The engineering parameters, including the UCS, shear strength parameters, and permeability, are correlated to the calcium carbonate content (CCC) for MICP or the biopolymer content (BPC) for BPT. Herein, simple empirical models with the fitting parameters are suggested. Particularly, it is noted that the different mechanisms of MICP and BPT lead to the distinctive features in properties. Although the simple correlations by using CCC or BPC can provide rough baseline estimates for the properties of treated sandy soils, nevertheless, development of more generic formulations that convolute other affecting factors remains unresolved.

Accordingly, each method can be applied to specific engineering practices. MICP treatment is presumed to induce strength improvement, while maintaining permeability up to a certain CCC value. Thus, MICP can be utilized as a method for permeating grouting in coarse sands. Further, it can also be used for liquefaction mitigation because MICP-treated sands can maintain hydraulic conductivity, thereby allowing the dissipation of excess pore water during seismic loading. On the other hand, it can be seen that BPT can increase strength and reduce permeability with a BPC lower than 2–3%. Thus, it can be used to construct water-sealing layers or hydraulic barriers in geotechnical practices. Owing to its high viscosity when mixed with water and soil grains, it can also be utilized as a grout material in compaction grouting or deep cement mixing (DCM) methods. However, to be practically and economically applicable at in situ fields, various factors such as workability, cost, proper equipment, and environmental issue need to be further assessed.

Declaration of Competing Interest

The authors declare that they have no known competing financial interests or personal relationships that could have appeared to influence the work reported in this paper.

Acknowledgements

This research was supported by a grant from 'Development of liquefaction damage prediction visualization system and liquefaction reinforcement method with high efficiency and low cost' funded by The Korea Institute of Civil Engineering and Building Technology, and by a grant (19CTAP-C151917-01) from Technology Advancement Research Program (TARP) funded by Ministry of Land, Infrastructure and Transport (MOLIT) of the Korean government. T.H. Kwon was also supported by the Rector-funded Visiting Fellowship (RFVF) Scheme of UNSW Canberra for collaborative research between UNSW and KAIST in July-August 2018.

References

[1] V. Achal, A. Mukherjee, M.S. Reddy, Microbial concrete: way to enhance the durability of building structures, J. Mater. Civ. Eng. 23 (6) (2011) 730–734.
[2] S.-G. Choi, S. Wu, J. Chu, Biocementation for sand using an eggshell as calcium source, J. Geotech. Geoenviron. Eng. 142 (10) (2016) 06016010.
[3] T. Bremner, P. Eng, Environmental aspects of concrete: problems and solutions, All-Russian Conference on Concrete and Reinforced Concrete, 2001.
[4] E. Worrell, L. Price, N. Martin, C. Hendriks, L.O. Meida, Carbon dioxide emissions from the global cement industry, Annu. Rev. Energy Env. 26 (1) (2001) 303–329.
[5] B. Petroleum, Statistical review of world energy 2009, BP, London, 2009.
[6] L.A. van Paassen, C.M. Daza, M. Staal, D.Y. Sorokin, W. van der Zon, M.C.M. van Loosdrecht, Potential soil reinforcement by biological denitrification, Ecol. Eng. 36 (2) (2010) 168–175.
[7] J.T. DeJong, K. Soga, E. Kavazanjian, S. Burns, L.A.V. Paassen, A.A. Qabany, A. Aydilek, S.S. Bang, M. Burbank, L.F. Caslake, C.Y. Chen, X. Cheng, J. Chu, S. Ciurli, A. Esnault-Filet, S. Fauriel, N. Hamdan, T. Hata, Y. Inagaki, S. Jefferis, M. Kuo, L. Lalaoui, J. Larrahondo, D.A.C. Manning, B. Martinez, B.M. Montoya, D.C. Nelson, A. Palomino, P. Renforth, J.C. Santamarina, E.A. Seagren, B. Tanyu, M. Tsesarsky, T. Weaver, Biogeochemical processes and geotechnical applications: progress, opportunities and challenges, Géotechnique 63 (4) (2013) 287–301.
[8] S.G. Choi, J. Chu, R.C. Brown, K. Wang, Z. Wen, Sustainable biocement production via microbially induced calcium carbonate precipitation: use of limestone and acetic acid derived from pyrolysis of lignocellulosic biomass, ACS Sustainable Chem. Eng. 5 (6) (2017) 5183–5190.
[9] M.P. Harkes, L.A. Van Paassen, J.L. Booster, V.S. Whiffin, M.C. van Loosdrecht, Fixation and distribution of bacterial activity in sand to induce carbonate precipitation for ground reinforcement, Ecol. Eng. 36 (2) (2010) 112–117.
[10] Y. Inagaki, M. Tsukamoto, H. Mori, S. Nakajiman, T. Sasaki, S. Kawasaki, A centrifugal model test of microbial carbonate precipitation as liquefaction countermeasure, Jiban Kogaku Janaru 6 (2) (2011) 157–167.
[11] B.M. Montoya, J.T. DeJong, R.W. Boulanger, Dynamic response of liquefiable sand improved by microbial-induced calcite precipitation, Géotechnique 63 (2013) 302–312.
[12] S.C. Bang, S.H. Min, S.S. Bang, KGS Awards Lectures: application of microbiologically induced soil stabilization technique for dust suppression, Int. J. Geo-Eng. 3 (2) (2011) 27–37.
[13] V. Stabnikov, M. Naeimi, V. Ivanov, J. Chu, Formation of water-impermeable crust on sand surface using biocement, Cem. Concr. Res. 41 (11) (2011) 1143–1149.
[14] J. Chu, V. Ivanov, V. Sabnikov, B. Li, Microbial method for construction of an aquaculture pond in sand, Géotechnique 63 (10) (2013) 871–875.
[15] S.-S. Park, S.-G. Choi, I.-H. Nam, Effect of plant-induced calcite precipitation on the strength of sand, J. Mater. Civ. Eng. 26 (8) (2014) 06014017.
[16] N. Hamdan, E.K. Jr, Enzyme-induced carbonate mineral precipitation for fugitive dust control, Géotechnique 66 (7) (2016) 546–555.
[17] A. Dakhane, S. Das, H. Hansen, S. O'Donnell, F. Hanoon, A. Rushton, C. Perla, N. Neithalath, Crack healing in cementitious mortars using enzyme-induced carbonate precipitation: Quantification based on fracture response, J. Mater. Civ. Eng. 30 (4) (2018) 04018035.
[18] S.S. Bang, S. Bang, S. Frutiger, L.M. Nehl, B.L. Comes, Application of novel biological technique in dust suppression, 2009, pp. (No. 09-0831).
[19] B. Knorr, Enzyme-induced carbonate precipitation for the mitigation of fugitive dust, Arizona State University, 2014.

[20] R. Dilrukshi, S. Kawasaki, Effective use of plant-derived urease in the field of geoenvironmental, Geotechnical Engineering. J Civil Environ Eng 6 (207) (2016) 2.
[21] J. Geotech. Geoenviron. Eng. 144 (11) (2018) 04018081, https://doi.org/10.1061/(ASCE)GT.1943-5606.0001973.
[22] R.E. Lappan, H.S. Fogler, Leuconostoc mesenteroides growth kinetics with application to bacterial profile modification, Biotechnol. Bioeng. 43 (9) (1994) 865–873.
[23] T.-H. Kwon, J.B. Ajo-Franklin, High-frequency seismic response during permeability reduction due to biopolymer clogging in unconsolidated porous media, Geophysics 78 (6) (2013). EN117-EN127.
[24] D.-H. Noh, J.B. Ajo-Franklin, T.-H. Kwon, B. Muhunthan, P and S wave responses of bacterial biopolymer formation in unconsolidated porous media, J. Geophys. Res. Biogeosci. 121 (4) (2016) 1158–1177.
[25] S.-M. Ham, I. Chang, D.-H. Noh, T.-H. Kwon, B. Muhunthan, Improvement of surface erosion resistance of sand by microbial biopolymer formation, J. Geotech. Geoenviron. Eng. 144 (7) (2018) 06018004.
[26] W. Ma, Y. Han, W. Ma, H. Han, H. Zhu, C. Xu, K. Li, D. Wang, Enhanced nitrogen removal from coal gasification wastewater by simultaneous nitrification and denitrification (SND) in an oxygen-limited aeration sequencing batch biofilm reactor, Bioresour. Technol. 244 (2017) 84–91.
[27] I.M. Young, J.W. Crawford, Interactions and self-organization in the soil-microbe complex, Science 304 (5677) (2004) 1634–1637.
[28] J. Kim, H. Dong, J. Seabaugh, S.W. Newell, D.D. Eberl, Role of microbes in the smectite-to-illite reaction, Science 303 (5659) (2004) 830–832.
[29] J. Jass, S. Roberts, H. Lappin-Scott, Microbes and enzymes in biofilms, Enzymes in the Environment. Activity, Ecology and Applications, Marcel Dekker Inc., New York, USA, 2002, pp. 307–326.
[30] S.W. Taylor, P.R. Jaffé, Substrate and biomass transport in a porous medium, Water Resour. Res. 26 (9) (1990) 2181–2194.
[31] P. Baveye, P. Vandevivere, B.L. Hoyle, P.C. DeLeo, D.S. de Lozada, Environmental impact and mechanisms of the biological clogging of saturated soils and aquifer materials, Critical reviews in environmental science and technology 28 (2) (1998) 123–191.
[32] B.C. Dunsmore, C.J. Bass, H.M. Lappin-Scott, A novel approach to investigate biofilm accumulation and bacterial transport in porous matrices, Environ. Microbiol. 6 (2) (2004) 183–187.
[33] V. Rebata-Landa, J.C. Santamarina, Mechanical effects of biogenic nitrogen gas bubbles in soils, J. Geotech. Geoenviron. Eng. 138 (2) (2012) 128–137.
[34] J.K. Mitchell, J.C. Santamarina, Biological Considerations in Geotechnical Engineering, J. Geotech. Geoenviron. Eng. 131 (10) (2005) 1222–1233.
[35] J. He, J. Chu, V. Ivanov, Mitigation of liquefaction of saturated sand using biogas, Géotechnique 63 (4) (2013) 267–275.
[36] G. Sharma, S. Sharma, A. Kumar, H. Ala'a, M. Naushad, A.A. Ghfar, G.T. Mola, F. J. Stadler, Guar gum and its composites as potential materials for diverse applications: A review, Carbohydr. Polym. (2018).
[37] S.L. Larson, J.K. Newman, C.S. Griggs, M. Beverly, C.C. Nestler, Biopolymers as an Alternative to Petroleum-Based Polymers for Soil Modification, ESTCP ER-0920: Treatability Studies, Engineer Research And Development Center Vicksburg Ms Environmental Lab (2012).
[38] H.R. Khatami, B.C. O'Kelly, Improving mechanical properties of sand using biopolymers, J. Geotech. Geoenviron. Eng. 139 (8) (2012) 1402–1406.
[39] J. Nakamatsu, S. Kim, J. Ayarza, E. Ramírez, M. Elgegren, R. Aguilar, Eco-friendly modification of earthen construction with carrageenan: Water durability and mechanical assessment, Constr. Build. Mater. 139 (2017) 193–202.
[40] E. Boquet, A. Boronat, A. Ramos-Cormenzana, Production of Calcite (Calcium Carbonate) Crystals by Soil Bacteria is a General Phenomenon, Nature 246 (5434) (1973) 527–529.
[41] Z. Wang, N. Zhang, G. Cai, Y. Jin, N. Ding, D. Shen, Review of ground improvement using microbial induced carbonate precipitation (MICP), Mar. Georesour. Geotechnol. 35 (8) (2017) 1135–1146.
[42] S. Stocks-Fischer, J.K. Galinat, S.S. Bang, Microbiological precipitation of CaCO3, Soil Biol. Biochem. 31 (11) (1999) 1563–1571.
[43] Y. Al-Salloum, S. Hadi, H. Abbas, T. Almusallam, M. Moslem, Bio-induction and bioremediation of cementitious composites using microbial mineral precipitation–A review, Constr. Build. Mater. 154 (2017) 857–876.
[44] R. Siddique, N.K. Chahal, Effect of ureolytic bacteria on concrete properties, Constr. Build. Mater. 25 (10) (2011) 3791–3801.
[45] J.T. DeJong, B.M. Mortensen, B.C. Martinez, D.C. Nelson, Bio-mediated soil improvement, Ecol. Eng. 36 (2) (2010) 197–210.
[46] N.H. de Leeuw, S.C. Parker, Surface structure and morphology of calcium carbonate polymorphs calcite, aragonite, and vaterite: an atomistic approach, J. Phys. Chem. B 102 (16) (1998) 2914–2922.
[47] C. Rodriguez-Navarro, F. Jroundi, M. Schiro, E. Ruiz-Agudo, M.T. González-Muñoz, Influence of substrate mineralogy on bacterial mineralization of calcium carbonate: Implications in stone conservation, Appl. Environ. Microbiol. AEM (2012) 07044–7111.
[48] V.S. Whiffin, Microbial microbial carbonate precipitation as a soil improvement technique, Biological Sciences & Biotechnology, Murdoch, Australia, 2004.
[49] J. DeJong, M.B. Fritzges, K. Nüsslein, Microbially Induced Cementation to Control Sand Response to Undrained Shear, J. Geotech. Geoenviron. Eng. 132 (11) (2006) 1381–1392.
[50] A. Al Qabany, K. Soga, Effect of chemical treatment used in MICP on engineering properties of cemented soils, Géotechnique 63(4) (2013) 331.
[51] Q. Zhao, L. Li, C. Li, M. Li, F. Amini, H. Zhang, Factors affecting improvement of engineering properties of MICP-treated soil catalyzed by bacteria and urease, J. Mater. Civ. Eng. 26 (12) (2014) 04014094.
[52] S.-G. Choi, K. Wang, J. Chu, Properties of biocemented, fiber reinforced sand, Constr. Build. Mater. 120 (2016) 623–629.
[53] L.A. van Paassen, M. van Loosdrecht, M. Pieron, A. Mulder, D. Ngan-Tillard, T. Van der Linden, Strength and deformation of biologically cemented sandstone, ISRM Regional Symposium-EUROCK 2009, International Society for Rock Mechanics, 2009.
[54] M. Li, C. Fang, S. Kawasaki, V. Achal, Fly ash incorporated with biocement to improve strength of expansive soil, Sci. Rep. 8 (1) (2018) 2565.
[55] J. Chu, V. Ivanov, V. Stabnikov, B. Li, Microbial method for construction of an aquaculture pond in sand, Géotechnique 63 (10) (2013) 871–875.
[56] L. Cheng, M.A. Shahin, R. Cord-Ruwisch, Bio-cementation of sandy soil using microbially induced carbonate precipitation for marine environments, Géotechnique 64 (12) (2014) 1010–1013.
[57] L. Cheng, R. Cord-Ruwisch, M.A. Shahin, Cementation of sand soil by microbially induced calcite precipitation at various degrees of saturation, Can. Geotech. J. 50 (1) (2013) 81–90.
[58] A. Smith, M. Pritchard, S. Bashir, The reduction of the permeability of a lateritic soil through the application of microbially induced calcite precipitation, Natural, Resources (2017).
[59] N. Soon, L. Lee, T. Khun, H. Ling, Improvements in engineering properties of soils through microbial-induced calcite precipitation, KSCE J Civ Eng 17 (4) (2013) 718–728.
[60] N.-J. Jiang, K. Soga, M. Kuo, Microbially Induced Carbonate Precipitation for Seepage-Induced Internal Erosion Control in Sand-Clay Mixtures, J. Geotech. Geoenviron. Eng. (2016) 04016100.
[61] F. Meyer, S. Bang, S. Min, L. Stetler, S. Bang, Microbiologically-induced soil stabilization: application of Sporosarcina pasteurii for fugitive dust control, Geo-frontiers 2011: advances in geotechnical engineering, 2011, pp. 4002–4011.
[62] N.-J. Jiang, K. Soga, The applicability of microbially induced calcite precipitation (MICP) for internal erosion control in gravel–sand mixtures, Géotechnique 67 (1) (2017) 42–55.
[63] M. Maleki, S. Ebrahimi, F. Asadzadeh, M. Emami, Tabrizi, Performance of microbial-induced carbonate precipitation on wind erosion control of sandy soil, Int. J. Environ. Sci. Technol. 13 (3) (2016) 937–944.
[64] E. Salifu, E. MacLachlan, K.R. Iyer, C.W. Knapp, A. Tarantino, Application of microbially induced calcite precipitation in erosion mitigation and stabilisation of sandy soil foreshore slopes: A preliminary investigation, Eng. Geol. 201 (2016) 96–105.
[65] Z. Han, X. Cheng, Q. Ma, An experimental study on dynamic response for MICP strengthening liquefiable sands, Earthquake Engineering and Engineering Vibration 15 (4) (2016) 673–679.
[66] K. Feng, B.M. Montoya, Quantifying level of microbial-induced cementation for cyclically loaded sand, J. Geotech. Geoenviron. Eng. 143 (6) (2017) 06017005.
[67] M. Burbank, T. Weaver, R. Lewis, T. Williams, B. Williams, R. Crawford, Geotechnical Tests of Sands Following Bioinduced Calcite Precipitation Catalyzed by Indigenous Bacteria, J. Geotech. Geoenviron. Eng. 139 (6) (2013) 928–936.
[68] A. Al Qabany, K. Soga, C. Santamarina, Factors affecting efficiency of microbially induced calcite precipitation, J. Geotech. Geoenviron. Eng. 138 (8) (2012) 992–1001.
[69] N.W. Soon, L.M. Lee, T.C. Khun, H.S. Ling, Factors affecting improvement in engineering properties of residual soil through microbial-induced calcite precipitation, J. Geotech. Geoenviron. Eng. 140 (5) (2014) 04014006.
[70] A. Sharma, R. Ramkrishnan, Study on effect of microbial induced calcite precipitates on strength of fine grained soils, Perspect. Sci. 8 (2016) 198–202.
[71] Y. Zhang, H. Guo, X. Cheng, Influences of calcium sources on microbially induced carbonate precipitation in porous media, Mater. Res. Innovat. 18 (sup2) (2014). S2-79-S2-84.
[72] S.-G. Choi, S. Wu, J. Chu, Biocementation for Sand Using an Eggshell as Calcium Source, J. Geotech. Geoenviron. Eng. (2016) 06016010.
[73] L. Cheng, M.A. Shahin, D. Mujah, Influence of Key Environmental Conditions on Microbially Induced Cementation for Soil Stabilization, J. Geotech. Geoenviron. Eng. (2016) 04016083.
[74] V. Rebata-Landa, Microbial activity in sediments: effects on soil behavior, Georgia Institute of Technology (2007).
[75] I. Hammad, F. Talkhan, A. Zoheir, Urease activity and induction of calcium carbonate precipitation by Sporosarcina pasteurii NCIMB 8841, Journal of Applied Sciences Research 9 (3) (2013) 1525–1533.
[76] F.G. Ferris, V. Phoenix, Y. Fujita, R.W. Smith, Kinetics of calcite precipitation induced by ureolytic bacteria at 10 to 20°C in artificial groundwater, Geochim. Cosmochim. Acta 68 (8) (2004) 1701–1710.
[77] A. Zamani, B.M. Montoya, Shearing and hydraulic behavior of MICP treated silty sand, Geotechnical Frontiers 2017, pp. 290-299.
[78] S.G. Choi, J. Chu, T.H. Kwon, Effect of chemical concentrations on strength and crystal size of biocemented sand, Geomechanics and Engineering 17 (5) (2019) 465–473.
[79] H.A. Keykha, B.B. Huat, A. Asadi, Electrokinetic stabilization of soft soil using carbonate-producing bacteria, Geotech. Geol. Eng. 32 (4) (2014) 739–747.
[80] F.J. Kadhim, J.-J. Zheng, INFLUENCES OF CALCIUM SOURCES AND TYPE OF SAND ON MICROBIAL INDUCED CARBONATE PRECIPITATION, International Journal of Advances in Engineering & Technology 10 (1) (2017) 20.

[81] M. Li, L. Li, U. Ogbonnaya, K. Wen, A. Tian, F. Amini, Influence of fiber addition on mechanical properties of MICP-treated sand, J. Mater. Civ. Eng. 28 (4) (2015) 04015166.
[82] M.L. Lee, W.S. Ng, Y. Tanaka, Stress-deformation and compressibility responses of bio-mediated residual soils, Ecol. Eng. 60 (2013) 142–149.
[83] V.S. Whiffin, L.A. van Paassen, M.P. Harkes, Microbial carbonate precipitation as a soil improvement technique, Geomicrobiol J. 24 (5) (2007) 417–423.
[84] L.A. van Paassen, R. Ghose, T.J. van der Linden, W.R. van der Star, M.C. van Loosdrecht, Quantifying biomediated ground improvement by ureolysis: large-scale biogrout experiment, J. Geotech. Geoenviron. Eng. 136 (12) (2010) 1721–1728.
[85] C. Shanahan, B. Montoya, Strengthening coastal sand dunes using microbial-induced calcite precipitation, Geo-Congress, Geo-characterization and Modeling for Sustainability 2014 (2014) 1683–1692.
[86] T. Danjo, S. Kawasaki, Microbially induced sand cementation method using Pararhodobacter sp. strain SO1, inspired by beachrock formation mechanism, Mater. Trans. 57 (3) (2016) 428–437.
[87] M.G. Gomez, J.T. DeJong, Engineering properties of bio-cementation improved sandy soils, Grouting 2017, pp. 23–33.
[88] G.G.N.N. Amarakoon, S. Kawasaki, Factors Affecting Sand Solidification Using MICP with Pararhodobacter sp, Mater. Trans. (2017) M-M2017849.
[89] M. Li, K. Wen, Y. Li, L. Zhu, Impact of oxygen availability on microbially induced calcite precipitation (MICP) treatment, Geomicrobiol J. 35 (1) (2018) 15–22.
[90] N.C. Consoli, M.A. Vendruscolo, A. Fonini, F. Dalla Rosa, Fiber reinforcement effects on sand considering a wide cementation range, Geotext. Geomembr. 27 (3) (2009) 196–203.
[91] B.M. Montoya, J.T. DeJong, Stress-strain behavior of sands cemented by microbially induced calcite precipitation, J. Geotech. Geoenviron. Eng. 141 (6) (2015) 04015019.
[92] R. Omar, R. Roslan, I. Baharuddin, M. Hanafiah, Micaceous Soil Strength and Permeability Improvement Induced by Microbacteria from Vegetable Waste, IOP Conference Series: Materials Science and Engineering, IOP Publishing (2016) 012083.
[93] Z. Kaltenbacher, M.I. Máté, L. Kopenetz, V. Farcas, I.C. Molnar, Synthesis of research on biogrout soil improvement method, Constructii 15 (2) (2014) 89.
[94] R. Saffari, G. Habibagahi, E. Nikooee, A. Niazi, Biological stabilization of a swelling fine-grained soil: The role of microstructural changes in the shear behavior, Iranian Journal of Science and Technology, Transactions of Civil Engineering 41 (4) (2017) 405–414.
[95] H. Canakci, W. Sidik, I. Halil Kilic, Effect of bacterial calcium carbonate precipitation on compressibility and shear strength of organic soil, Soils Found. 55 (5) (2015) 1211–1221.
[96] K. Feng, B. Montoya, Influence of Confinement and Cementation Level on the Behavior of Microbial-Induced Calcite Precipitated Sands under Monotonic Drained Loading, J. Geotech. Geoenviron. Eng. 142 (1) (2015) 04015057.
[97] M.-J. Cui, J.-J. Zheng, R.-J. Zhang, H.-J. Lai, J. Zhang, Influence of cementation level on the strength behaviour of bio-cemented sand, Acta Geotech. 12 (5) (2017) 971–986.
[98] L. Cheng, R. Cord-Ruwisch, Upscaling effects of soil improvement by microbially induced calcite precipitation by surface percolation, Geomicrobiol J. 31 (5) (2014) 396–406.
[99] L.A. Van Paassen, Biogrout, ground improvement by microbial induced carbonate precipitation, None (EN), Delft University of Technology, TU Delft, 2009.
[100] V. Ivanov, J. Chu, V. Stabnikov, J. He, M. Naeimi, Iron-based bio-grout for soil improvement and land reclamation, Proceedings of the 2nd International Conference on Sustainable Construction Materials and Technologies, Italy, 2010, pp. 415–420.
[101] K. Muthukkumaran, B.S. Shashank, Durability of microbially induced calcite precipitation (micp) treated cohesionless soils, Japanese Geotechnical Society Special Publication 2 (56) (2016) 1946–1949.
[102] L. Cheng, M. Shahin, Bacteria induced cementation for soil stabilization, in: Proceedings of the 19th International Conference on Soil Mechanics and Geotechnical Engineering, 2017, pp. 2371–2374.
[103] D. Mujah, M.A. Shahin, L. Cheng, State-of-the-art review of biocementation by microbially induced calcite precipitation (MICP) for soil stabilization, Geomicrobiol J. 34 (6) (2017) 524–537.
[104] S. Kalia, L. Averous, Biopolymers: Biomedical and Environmental Applications, Wiley, 2011.
[105] I. Chang, J. Im, G.C. Cho, Introduction of microbial biopolymers in soil treatment for future environmentally-friendly and sustainable geotechnical engineering, Sustainability 8 (3) (2016) 251.
[106] S. Dumitriu, Polymeric biomaterials, 2nd ed., Marcel Dekker Inc, New York, 2002.
[107] A. Clark, S. Ross-Murphy, Structural and mechanical properties of biopolymer gels, Biopolymers, Springer, Berlin Heidelberg (1987) 57–192.
[108] W.M. Kulicke, H. Nottelmann, Structure and Swelling of Some Synthetic, Semisynthetic, and Biopolymer Hydrogels, Polymers in Aqueous Media, American Chemical Society, Washington, DC, 1989, pp. 15-44.
[109] A. Imeson, Food stabilisers, thickeners and gelling agents, Wiley-Blackwell Pub., Chichester, U.K.; Ames, Iowa, 2010.
[110] D.M. Kirchmajer, B. Steinhoff, H. Warren, R. Clark, M. in het Panhuis, Enhanced gelation properties of purified gellan gum, Carbohydr. Res. 388 (2014) 125–129.
[111] H. Izawa, J.-I. Kadokawa, Preparation and characterizations of functional ionic liquid-gel and hydrogel materials of xanthan gum, J. Mater. Chem. 20 (25) (2010) 5235–5241.
[112] H. Hassan, S. Al-Oraimi, R. Taha, Evaluation of open-graded friction course mixtures containing cellulose fibers and styrene butadiene rubber polymer, J. Mater. Civ. Eng. 17 (4) (2005) 416–422.
[113] J. Daniel, R.L. Whistler, A.C.J. Voragen, W. Pilnik, Starch and other polysaccharides, VCH Verlagsgesellschaft mbH, Weinheim, Ullmann's Encyclopedia of Industrial Chemistry, 1994.
[114] M.W. Wan, I.G. Petrisor, H.T. Lai, D. Kim, T.F. Yen, Copper adsorption through chitosan immobilized on sand to demonstrate the feasibility for in situ soil decontamination, Carbohydr. Polym. 55 (3) (2004) 249–254.
[115] G.C. Barrére, C.E. Barber, M.J. Daniels, Molecular cloning of genes involved in the production of the extracellular polysaccharide xanthan by Xanthomonas campestris pv. campestris, Int. J. Biol. Macromol. 8 (6) (1986) 372–374.
[116] J.T. Oliveira, L. Martins, R. Picciochi, P.B. Malafaya, R.A. Sousa, N.M. Neves, J.F. Mano, R.L. Reis, Gellan gum: a new biomaterial for cartilage tissue engineering applications, J. Biomed. Mater. Res. Part A 93 (3) (2010) 852–863.
[117] A.P. Imeson, Thickening and gelling agents for food, Springer Science & Business Media, 2012.
[118] M. McIntosh, B.A. Ston, V.A. Stanisich, Curdlan and other bacterial (1->3)-beta-D-glucans, Applied Microbiol. Biotechnol. 68 (2) (2005) 163–173.
[119] A. Bacic, G.B. Fincher, B.A. Stone, Chemistry, biochemistry, and biology of (1–3)-[beta]-glucans and related polysaccharides, 1st, ed, Academic, Amsterdam, 2009.
[120] H.D. Shin, M.K. Son, B.R. Park, C.W. Son, H.J. Jang, Composition containing Beta-glucan for prevention and treatment of osteoporosis, in: D.D. Mckay (Ed.) Glucan Corporation, United States, 2004, p. 6.
[121] I. Chang, G.-C. Cho, Shear strength behavior and parameters of microbial gellan gum-treated soils: from sand to clay, Acta Geotech. (2018) 1–15.
[122] I. Chang, G.-C. Cho, Strengthening of Korean residual soil with β-1,3/1,6-glucan biopolymer, Constr. Build. Mater. 30 (2012) 30–35.
[123] I. Chang, J. Im, G.-C. Cho, Geotechnical engineering behaviors of gellan gum biopolymer treated sand, Can. Geotech. J. (2016) 1–13.
[124] I. Chang, A.K. Prasidhi, J. Im, G.-C. Cho, Soil strengthening using thermo-gelation biopolymers, Constr. Build. Mater. 77 (2015) 430–438.
[125] Y. Kulshreshtha, E. Schlangen, H. Jonkers, P. Vardon, L. Van Paassen, CoRncrete: A corn starch based building material, Constr. Build. Mater. 154 (2017) 411–423.
[126] H. Fatehi, S.M. Abtahi, H. Hashemolhosseini, S.M. Hejazi, A novel study on using protein based biopolymers in soil strengthening, Constr. Build. Mater. 167 (2018) 813–821.
[127] N. Latifi, S. Horpibulsuk, C.L. Meehan, M.Z. Abd Majid, M.M. Tahir, E.T. Mohamad, Improvement of problematic soils with biopolymer—an environmentally friendly soil stabilizer, J. Mater. Civ. Eng. 29(2) (2016) 04016204.
[128] N. Latifi, S. Horpibulsuk, C.L. Meehan, M.Z.A. Majid, A.S.A. Rashid, Xanthan gum biopolymer: an eco-friendly additive for stabilization of tropical organic peat, Environmental Earth Sciences 75 (9) (2016) 825.
[129] M.K. Ayeldeen, A.M. Negm, M.A. El Sawwaf, Evaluating the physical characteristics of biopolymer/soil mixtures, Arabian J. Geosci. 9 (5) (2016) 1–13.
[130] N. Hataf, P. Ghadir, N. Ranjbar, Investigation of soil stabilization using chitosan biopolymer, J. Cleaner Prod. 170 (2018) 1493–1500.
[131] I. Chang, J. Im, M.-K. Chung, G.-C. Cho, Bovine casein as a new soil strengthening binder from diary wastes, Constr. Build. Mater. 160 (2018) 1–9.
[132] R.A. Nugent, G. Zhang, R.P. Gambrell, Effect of exopolymers on the liquid limit of clays and its engineering implications, Transp. Res. Rec. 2101 (2009) 34–43.
[133] R. Chen, L. Zhang, M. Budhu, Biopolymer stabilization of mine tailings, J. Geotech. Geoenviron. Eng. 139 (10) (2013) 1802–1807.
[134] I. Chang, G.-C. Cho, Geotechnical behavior of a beta-1,3/1,6-glucan biopolymer-treated residual soil, Geomechanics and Engineering 7 (6) (2014) 633–647.
[135] I. Chang, Y.-M. Kwon, J. Im, G.-C. Cho, Soil consistency and inter-particle characteristics of xanthan gum biopolymer containing soils with pore-fluid variation, Can. Geotech. J. (2018).
[136] E. Kavazanjian, E. Iglesias, I. Karatas, Biopolymer soil stabilization for wind erosion control, in: M. Hamza, M. Shahien, Y. El-Mossallamy (Eds.), the 17th International Conference on Soil Mechanics and Geotechnical Engineering IOS Press, Alexandria, Egypt, 2009, pp. 881–884.
[137] W.J. Orts, R.E. Sojka, G.M. Glenn, Biopolymer additives to reduce erosion-induced soil losses during irrigation, Ind. Crops Prod. 11 (1) (2000) 19–29.
[138] S. Larson, J. Ballard, C. Griggs, J.K. Newman, C. Nestler, An innovative non-ptroleum Rhizobium Tropici biopolymer salt for soil stabilization, ASME 2010 International Mechanical Engineering Congress and Exposition, American Society of Mechanical Engineers, Vancouver, Canada, 2010, pp. 1279-1284.
[139] I. Chang, A.K. Prasidhi, J. Im, H.-D. Shin, G.-C. Cho, Soil treatment using microbial biopolymers for anti-desertification purposes, Geoderma 253 (2015) 39–47.
[140] J. Plank, Applications of biopolymers in construction engineering, Biopolymers Online, Wiley-VCH Verlag GmbH & Co. KGaA, 2005.
[141] J. Peralta, M.A. Raouf, S. Tang, R.C. Williams, Bio-Renewable Asphalt Modifiers and Asphalt Substitutes, in: K. Gopalakrishnan, J. van Leeuwen, R.C. Brown

(Eds.), Sustainable Bioenergy and Bioproducts: Value Added Engineering Applications, Springer, London, London, pp. 89–115.
[142] E. Miękoś, M. Zieliński, K. Kołodziejczyk, M. Jaksender, Application of industrial and biopolymers waste to stabilise the subsoil of road surfaces, Road Materials and Pavement Design (2017) 1–14.
[143] A. Bouazza, W. Gates, P. Ranjith, Hydraulic conductivity of biopolymer-treated silty sand, Géotechnique 59 (1) (2009) 71–72.
[144] R. Khachatoorian, I.G. Petrisor, C.-C. Kwan, T.F. Yen, Biopolymer plugging effect: laboratory-pressurized pumping flow studies, J. Petrol. Sci. Eng. 38 (1–2) (2003) 13–21.
[145] A.M. Al-Darby, The hydraulic properties of a sandy soil treated with gel-forming soil conditioner, Soil Technology 9 (1–2) (1996) 15–28.
[146] J. Im, A.T.P. Tran, I. Chang, G.-C. Cho, Dynamic properties of gel-type biopolymer-treated sands evaluated by Resonant Column (RC) tests, Geomechanics and Engineering 12 (5) (2017) 815–830.
[147] S. Smitha, A. Sachan, Use of agar biopolymer to improve the shear strength behavior of sabarmati sand, Int. J. Geotech. Eng. 10 (4) (2016) 387–400.
[148] N. Akbulut, A.F. Cabalar, Effects of Biopolymer on Some Geotechnical Properties of a Sand, New Frontiers in Geotechnical Engineering - Geotechnical Special Publications 243, ASCE, Shanghai, China, 2014, pp. 28–37.
[149] I. Chang, J. Im, A.K. Prasidhi, G.-C. Cho, Effects of Xanthan gum biopolymer on soil strengthening, Constr. Build. Mater. 74 (2015) 65–72.
[150] R. Chen, D. Ramey, E. Weiland, I. Lee, L. Zhang, Experimental investigation on biopolymer strengthening of mine tailings, J. Geotech. Geoenviron. Eng. 142 (12) (2016) 06016017.
[151] M.U. Qureshi, I. Chang, K. Al-Sadarani, Strength and durability characteristics of biopolymer-treated desert sand, Geomechanics and Engineering 12 (5) (2017) 785–801.
[152] A.F. Cabalar, M. Wiszniewski, Z. Skutnik, Effects of Xanthan Gum Biopolymer on the Permeability, Odometer, Unconfined Compressive and Triaxial Shear Behavior of a Sand, Soil Mech. Found. Eng. 54 (5) (2017) 356–361.
[153] M. Wiszniewski, Z. Skutnik, M. Biliniak, A.F. Çabalar, Some geomechanical properties of a biopolymer treated medium sand, Annals of Warsaw University of Life Sciences–SGGW, Land Reclamation 49 (3) (2017) 201–212.
[154] J. Liu, Y. Bai, Z. Song, Y. Lu, W. Qian, D.P. Kanungo, Evaluation of strength properties of sand modified with organic polymers, Polymers 10 (3) (2018) 287.
[155] S. Lee, I. Chang, M.-K. Chung, Y. Kim, J. Kee, Geotechnical shear behavior of xanthan gum biopolymer treated sand from direct shear testing, Geomechanics and Engineering 12 (5) (2017) 831–847.
[156] M. Wiszniewski, A.F. Cabalar, Hydraulic conductivity of a biopolymer treated sand, New Frontiers in Geotechnical Engineering (2014) 19–27.
[157] S.K. Tiwari, J.P. Sharma, J.S. Yadav, Behavior of dune sand and its stabilization techniques, Journal of Advanced Research in Applied Mechanics 19 (1) (2016) 1–15.